FORMATION OF NANODIMENSIONAL LAYER OF CATALYTICALLY ACTIVE METALS ON STAINLESS STEEL SURFACE BY IONIC IMPLANTATION

V. A. Zazhigalov,[1] V. V. Honcharov,[2] I. V. Bacherikova,[1] R. Socha,[3] and J. Gurgul[3]

It was shown by XRD, thin-layer XRD, SEM, and XPS that ionic implantation of Mo, Ni, and Ti on the surface of stainless steel (SS) leads to the formation of a layer of implants 80-100 nm thick on the SS surface with partial penetration of the implant in the surface layer to a depth of 20-50 nm. It was found that the mechanical properties and thermal stability of the composites depend on the presence of such a subsurface layer. The possibility of using the composites in catalysis and photocatalysis is discussed.

***Key words**: ionic implantation, stainless steel, catalysts.*

Catalysts deposited on metallic supports have a series of advantages compared with their analogs based on ceramics. This is mainly due to the nature of the support, which secures high mechanical and thermal stability, thermal conductivity, electric conductivity, and at the same time the possibility of changing the form of the prepared catalyst in relation to the scale and design of the reactor. The prospect of using foil as metallic support depends both on its small thickness compared to other scale factors and on the possibility of corrugation and twisting (the production of an analog of a block ceramic) and simple variation of its geometric dimensions even after deposition of the layer of catalytically active elements.

The difficulty in the production of such catalysts comes from problems that arise during the synthesis of a layer of active components with good adhesion to the metal (support) on the surface of the support in order to ensure good mechanical and thermal stability. The various methods for chemical or electrochemical deposition of the active components on the surface of a metallic support, including CVD and PVD, do not ensure sufficiently strong bond to the support [1]. When they are used a surface layer with thermophysical properties that differ from metallic support is formed, leading to detachment at the high exploitation temperatures.

A method for the formation of a sufficiently porous initial layer (undercoat, most often aluminum oxide) on which the catalytically active elements were then deposited was used in order to solve the problems of small surface area and lack of

---
[1]Institute for Sorption and Problems of Endoecology, National Academy of Sciences of Ukraine, Vul. Henerala Naumova, 13, Kyiv 03164, Ukraine. E-mail: zazhigal@ispe.kiev.ua.
[2]State Establishment "Lugansk State Medical University," Vul. Budivel'nykiv, 32, Rubizhne 93012, Lugans'ka Obl., Ukraine.
[3]Jerzy Haber Institute of Catalysis and Surface Chemistry PAS, Niezapominajek, 8, Krakow PL-3023, Poland.

porous structure in the metallic supports (like ceramic supports) [1]. In this case, however, the different thermal expansion coefficients of the metal (support) and the undercoat often lead to detachment of the latter.

A promising method for the production of catalysts on metallic supports is low-temperature implantation, where the active component in not only deposited on the surface but enters the surface layer [2]. The intermediate layer formed in this way can provide a smooth transition from the support itself to the layer of catalytically active components.

There are no published data on the use of this method in the synthesis of deposited catalysts, but there are limited data on investigation of the physicochemical characteristics of the synthesized composites. However, it should be noted that low-temperature ionic implantation has been used to strengthen articles based on various types of steel [3-5]. A development of no lesser interest could be use of this method for the production of a thin-layer coating of elements and their combinations on the surface of such supports as ceramics, silicon, silicon carbide, etc., used in modern technologies and particularly in micro- and nanoelectronics and LED technology. The method may prove useful for the creation of a new generation of photocatalysts on formed supports since the use of highly dispersed catalysts has a series of obvious disadvantages (including technological ones). They include reduced penetration of cloudy dispersions for irradiation, the high recombination rate of electron/hole pairs, the substantial cost of the separation of solid particles from the substrate, the periodicity of the process, etc.

It is clear that these developments cannot be pursued without a knowledge of data on the various properties of the synthesized composites and the effect of the synthesis parameters on them. Data from investigation into the properties of samples obtained by ionic implantation using stainless steel foil as support are presented in the present report.

EXPERIMENTAL

Composites based on stainless steel 12Cr18Ni10Ti foil (thickness 80 μm) were produced in the implantation apparatus described in [6]. During the synthesis Mo, Ni, Ti, and Al were used as implants. Cathode sputtering of the target (one of the metals) with the ions of an auxiliary gas (nitrogen) was used. The implantation energy was 20 keV. X-ray diffraction analysis (XRD) of the samples was performed on Philips PW 1830 diffractometer (CuK_α radiation, monochromator). A Rigaku D/MAX RAPID two-dimensional X-ray diffractometer with an incident angle of 5° (XRD-TF) was used to investigate the thin surface layers. The specific surface area of the composites was determined by the adsorption of krypton on a NOVA 2200e instrument (Quantachrome Instruments). The surface morphology of the samples was investigated on a Hitachi S-400 scanning electron microscope (SEM) and a NanoScope Multi Mode V atomic-force microscope (AFM), and the results were processed with WSxM 4.0 (Version 13.0) software. The surface composition was investigated by X-ray photoelectron spectroscopy (XPS) on a spectrometer fitted with a hemispherical analyzer (SES R4000, Gammadata Scienta) and calibrated according to ISO 15472:2001. The spectra were analyzed with CasaXPS 2.3.10 software. The standard for determination of the electron energy was the C1s line (285.0 eV). The depth distribution of elements for the composites based on stainless steel foil was investigated by XPS (ESCA-3, VG Scientific) by removing layers by bombardment with argon. The strength of the bond between the coating of active elements and the surface of the support was estimated by the sclerometric method [7]. The catalytic activity of the samples in gas-phase catalysis reactions was determined in flow-type apparatus with online chromatographic analysis of the products [8]. The photocatalytic characteristics of the composites were studied in a cylindrical reactor (diameter 10 cm) with the sample placed along the wall (implantation on two sides of the support) in the form of a tape 5 cm high and a submerged radiation source (at the center of the reactor). Samples for analysis were taken with a microsyringe and analyzed on a Khrom-2 chromatograph (Selmi) by analogy with [9].

RESULTS AND DISCUSSION

Investigation of the samples by XRD [10] showed that, irrespective of the nature of the implanted metal, the diffractograms of all the composites only contain reflections of the (111), (200), and (220) planes of the austenite phase characteristic of the support (stainless steel). The reflection of the (220) plane has the highest intensity. Analogous results, indicating the absence of reflections from the implants, were obtained in [11-14] although the authors used larger energies and implantation doses. It should be noted that it was established in [11, 12] that implantation of Ag and Mo leads to some shift of
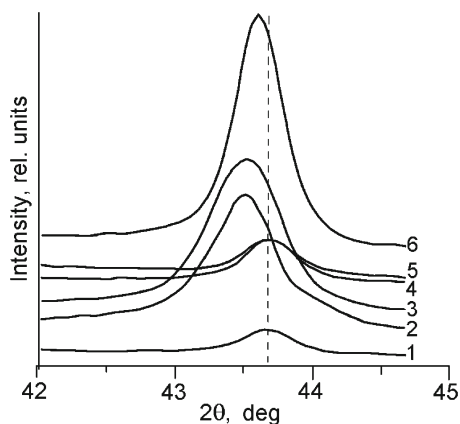
Fig. 1. Results of investigation of the composites by XRD-TF: 1) stainless steel support; 2) Ti/SS; 3) Mo/SS; 4) Al/SS; 5) Al/SS + HT; 6) Ni/SS.

the (111) and (220) reflections toward smaller angles, which results from entry of the ions into the structure of the stainless steel.

In view of the fact that we did not observe such changes (a smaller amount of the implanted element) by X-ray diffraction the composites were investigated by XRD-TF. It was established for all the samples that only reflections from the (111), (200), and (220) planes of the austenite phase were observed. However, implantation results in a change of their intensity, and the (111) reflection has maximum intensity for all the composites. At the same time, all the reflections are shifted toward smaller angles (with the exception of the implantation of Al). The largest shift was observed for the (111) plane (Fig. 1). Such changes in the intensity and position of the reflections may be due to their partial insertion into the subsurface layers of the stainless steel with some increase of the interplanar distance of the austenite. A similar effect was suggested by the authors in [11-14]. The absence of changes in the X-ray diffractograms for the implantation of Al may be due to the small ionic radius of the ion compared with the other studied metals or Ag [12].

By investigation of the synthesized composites by SEM it was possible to establish that a substantial change in the surface morphology of the stainless steel occurs as a result of implantation. An image of the cross-section of the samples showed that the implanted metals form a compact layer with thicknesses of 60-100 nm on the surface of the support [6, 15]. It should be noted that the thickness of this layer is significantly smaller than in the case of deposition of the elements on the surface of the metallic support by other methods (200-2000 nm) [16-20]. At the same time, the SEM data for the cross-section of the sample did not make it possible to establish the presence of a boundary (subsurface) layer of the support into which the ions of the implants had penetrated. This may be due both to the small depth of penetration of the metal ions into the stainless steel and to the resolving power of the method.

Theoretical calculation of the depth of penetration of the implants into the stainless steel was undertaken with the RIO software developed by the authors [21], the adequacy of which was checked by comparing the results with data obtained by the familiar SRIM-2012 and Gwyddion 2.31 methods in [10, 21]. The results for the composites studied in the present work are presented in Fig. 2a. As seen, the largest depth of penetration is observed for the aluminum ions, and the smallest for the molybdenum ions, which corresponds in general to the ionic radii of the metals. The results from experimental investigation of the depth of penetration of the implants by XPS are presented in Fig. 2b. Account must be taken of the fact that the thickness of the deposited layer of implant on the surface of the stainless steel in the experiment was taken as 80 nm, while the accuracy of determination of the depth of removal with argon (the thickness of the removed layer) was 2-4 nm. As seen from Fig. 2b, the experimental data confirm the results of the calculation fairly well. The curves for the variation of the implant content in the stainless steel (the right part after the zero point) practically agree with the calculated data (Fig. 2a). The results show that the maximum depth of penetration into the support is observed with aluminum, while the minimum is observed with molybdenum.
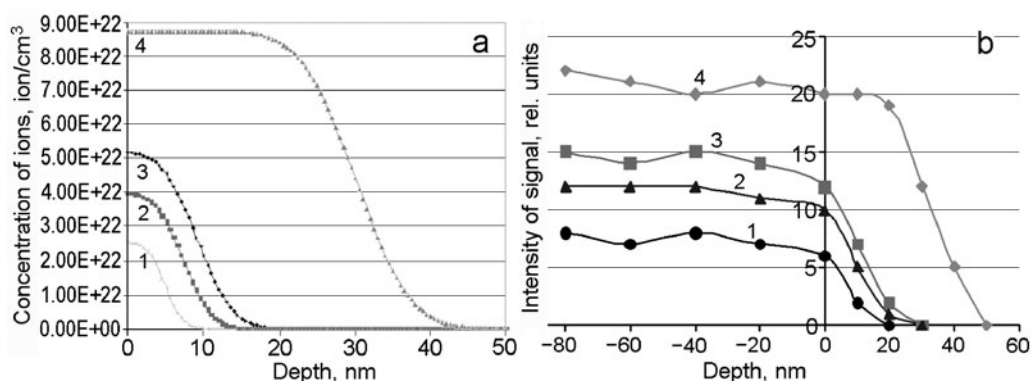
130

Fig. 2. Theoretical (a) and experimental (b) (XPS) investigation of the depth of penetration of the implant in the support: 1) Mo; 2) Ni; 3) Ti; 4) Al.

TABLE 1. Surface Parameters of the Synthesized Composites

Composite	$D \cdot 10^{16}$, ion/cm^2	Strength of surface layer, GPa		Coefficient of roughness			$S_{sp} \cdot 10^2$, m^2/g	
		Initial composite	After HT	Calculation		AFM	Initial composite	After HT
				RIO	Gwyddion			
SS	–	1.7	–	3.54	3.72	3.53	0.022-0.024	–
Al/SS	2.5	3.4	–	–	–	–	0.27	15
	5.0	5.7	3.8	4.87	4.78	5.21	0.45	26
Ni/SS	5.0	6.3	5.5	4.35	4.34	4.44	0.36	22
Ti/SS	2.5	3.1	–	–	–	–	0.25	14
	5.0	5.3	5.1	3.95	4.14	4.23	0.33	19
Mo/SS	2.5	5.7	–	–	–	–	0.17	10
	5.0	6.8	6.2	4.44	4.56	4.98	0.24	16
Al/SS*	–	1.5	0.9	–	–	–	0.09	5
Mo/SS**	–	0.7	–	–	–	–	0.21	9

Notes. D is the implantation dose; HT is heat treatment in air at 800 °C; SS is initial support, stainless steel; *Synthesized by plasma-chemical method; **Synthesized by electrochemical method.

These results thus confirm the previously made assumptions (based on XRD and XRD-TF) about the formation of an intermediate layer with implants introduced into the subsurface layer of the support.

The results from investigation of the mechanical strength of the surface of the synthesized composites are presented in Table 1. As seen from these data, the strength of the surface layer of all the composites at the micrometer depth of indentation (sclerometry), which is significantly greater than the thickness of the layer of implants, is higher than the strength of the initial support (stainless steel). This fact supports the long-range effect that has been described, for example, for silicon substrates
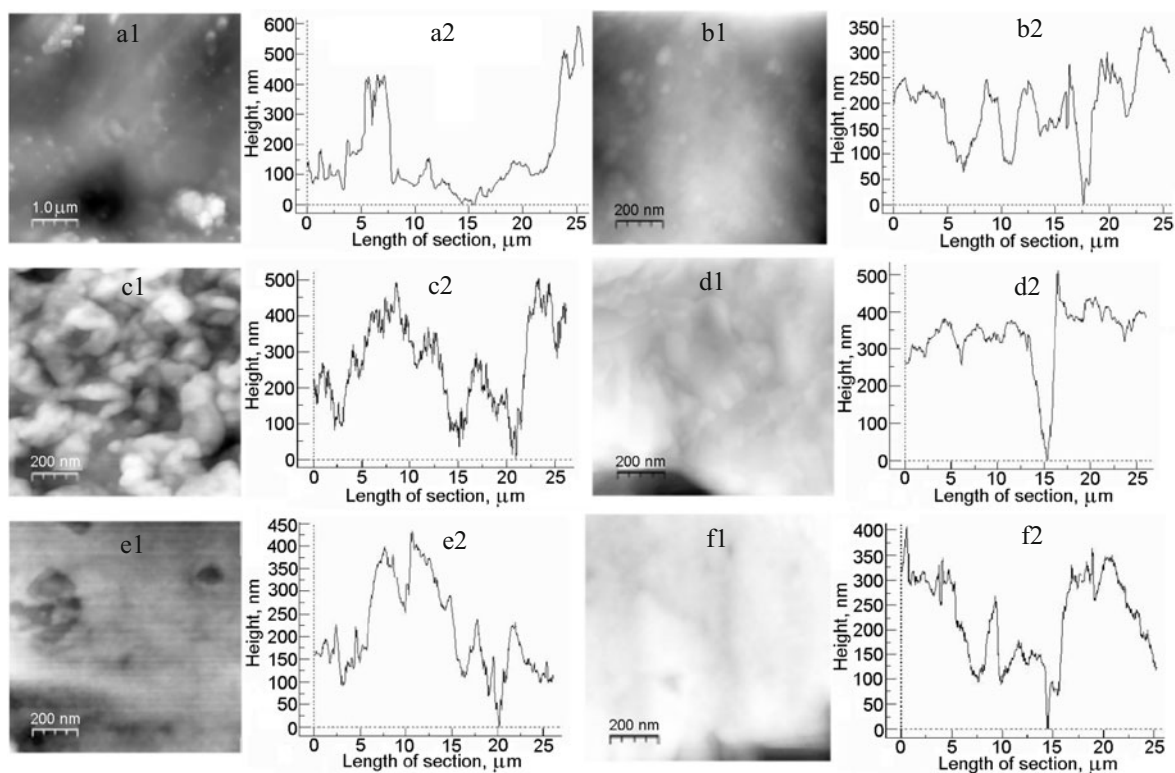
Fig. 3. Morphology of the surface of the composites according to AFM: a) stainless steel support; b) Al/SS; c) Al/SS + HT; d) Mo/SS; e) Ni/SS; f) Ti/SS. a1-f1) view of surface; a2-f2) surface profile.

[22]. Attention must be drawn to the fact that the strength of the surface layer of the samples synthesized by ionic implantation is higher than for the samples produced by plasma-chemical or electrochemical methods. The damage to the surface by the diamond indenter also differs in nature: for the composites synthesized by ionic implantation there is a scratch smooth and constant in width (plasticity), whereas for the sample produced by the plasma-chemical method the edge of the scratch is jagged in form. The highest value for the surface strength is obtained with the implantation of molybdenum. It was found that heat treatment of the composites reduces the strength of the surface layer to some degree. However, its value remains larger than for the stainless steel. The largest decrease of strength is observed in the composite with implanted aluminum, for which it was established [21] that its oxidation is accompanied by some increase in the thickness of the layer of implant on the surface of the support (to 130-150 nm). Here it should be noted that separation of the surface layer of implants from the surface of the support is not observed during bending (corrugation) both of the initial synthesized composites and of those formed after heat treatment, indicating a high breaking strength.

The data from AFM show that implantation of metal ions leads to a substantial change both in the general appearance of the stainless steel surface and in its morphology (Fig. 3). The surface profiles for the initial support presented in Fig. 3 are characterized by the presence of fairly deep (200-300 nm) and broad (up to 15 μm) depressions (cavities) as a result of the foil production technology. Implantation results in the formation of a surface layer of implants filling the broad cavities and forming both fairly narrow depressions 1-2 μm wide and macropores (diameter 50-100 nm), i.e., secondary porosity associated with the layer of implant. As seen from comparison of the data presented in Fig. 3, b2 and Fig. 3, c2, heat treatment leads to an increase in the number of pores. Implantation of metal ions also leads to increase in the surface roughness of the stainless steel (Table 1). As a result, the specific surface area of the stainless steel, which is practically equal to its geometric surface $(2.2\text{-}2.4)\cdot 10^{-4}$ m^2/g, is increased by more than an order of magnitude during implantation of the metal ions $(1.7\text{-}4.5)\cdot 10^{-3}$ m^2/g, while subsequent heat treatment of the sample leads to a further increase of the specific surface area by two orders of magnitude
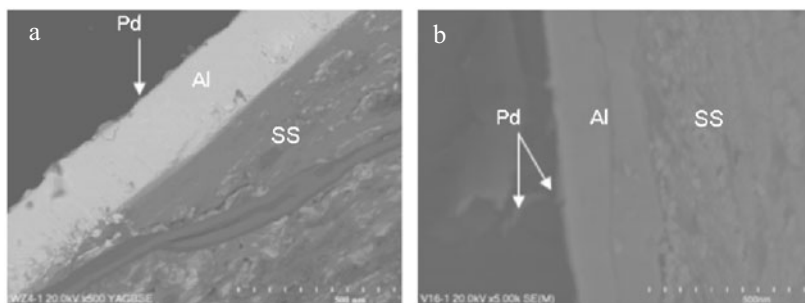
Fig. 4. SEM of cross-section of Pd/Al/SS catalyst after oxidation of methane:
a) Pd/Al/SS-IoIm; b) Pd/Al/SS-PCh.

(Table 1). It should be noted that the ionic implantation method makes it possible to increase the specific surface area of the stainless steel to a greater degree than other proposed methods [23-26] of increasing the surface area of the support.

As a result, as demonstrated in [27], the composite with implanted aluminum (after heat treatment) can be used for the synthesis of effective and thermally stable palladium- and platinum-containing catalysts by the traditional and simple impregnation method. During oxidation of methane under conditions of low temperatures and hydrocarbon concentrations such catalysts (Pd/Al/SS-IoIm) are somewhat inferior in their activity to the catalyst synthesized by the plasma-chemical method (Pd/Al/SS-PCh). However, with elevated concentrations of methane (modeling use in gas turbines or catalytic burners) both catalysts have equal activity [27]. Investigation of the samples after high-temperature oxidation of methane on them showed (Fig. 4) that for the Pd/Al/SS-IoIm sample the structures both of the layer of deposited palladium and of the implanted aluminum are preserved, whereas in the Pd/Al/SS-PCh sample partial separation of palladium and disruption of the structure of the intermediate layer are observed.

The first results obtained by XPS for a composite with implanted aluminum were published in [6, 10]. Data for some of the initial synthesized composites were analyzed in [27]. A detailed analysis of the XPS spectra for the initial composites and the samples after heat treatment is given below. Deconvolution of the spectrum of the C1s electrons into components shows the presence of three peaks with binding energies of 285, 286.6, and 288.5 eV, which belong to the condensed C–H groups (almost always present in the XP spectra and serving as standard for determining the bond energy of the electrons of the other elements), to the surface C–OH groups, and to the carbon attached to two oxygen atoms (the COOH groups), respectively. Such a spectrum is typical both of the initial support and of all the investigated composites. The form of the spectrum is not affected by the nature of the implant or by the heat treatment. Only the individual components in the spectrum of the C1s electrons are changed.

The typical form of the spectrum of the O1s electrons for the initial composites is shown in Fig 5, a1. The spectrum contains five peaks of which four with E_b 529.7-530.0, 531.6-531.8, 532.9-533.2, and 535.8-536.0 eV are characteristic of the oxide compounds of the various metals [28]. They indicate the presence of the oxygen of the oxide lattice, the C=O and Me=O groups, C–OH and Me–OH groups, and adsorbed oxygen in the form of O^{2-}, respectively. The intensity ratio of the peaks depends on the nature of the implant. The fifth peak with E_b = 527.6 eV may indicate the presence of additional transfer of electron density to the oxygen from the elements that enter the surface of the composite. Heat treatment of the composites leads to substantial changes in the spectrum of the O1s electrons (Fig. 5, a2). There are three peaks with electron bond energies of 529.7-529.9, 531.4-531.7, and 534.4-534.7 eV, which belong to the lattice oxygen, the C=O groups, and adsorbed molecular oxygen. The exception is the composite with implanted titanium, for which the low-intensity peak with E_b = 528.0 eV is retained.

A typical spectrum for the N1s electrons of the synthesized composites is presented in Fig. 5, b1. The spectrum contains three peaks, where the peak with E_b = 396.1-396.2 eV indicates the formation of nitrides of the implant metals (absent for the composite with implanted Mo). The peak with E_b = 398.2-398.4 eV indicates the presence of implanted nitrogen in the surface layer of the samples. The peak with bond energy greater than 400 eV is due to the formation of the oxynitrides of the metals with significant transfer of electron density from the nitrogen to the oxygen (N→O) [29]. The presence of this peak agrees well with the presence of a peak with E_b = 527.6 eV in the spectrum of the O1s electrons (see above). Heat treatment of
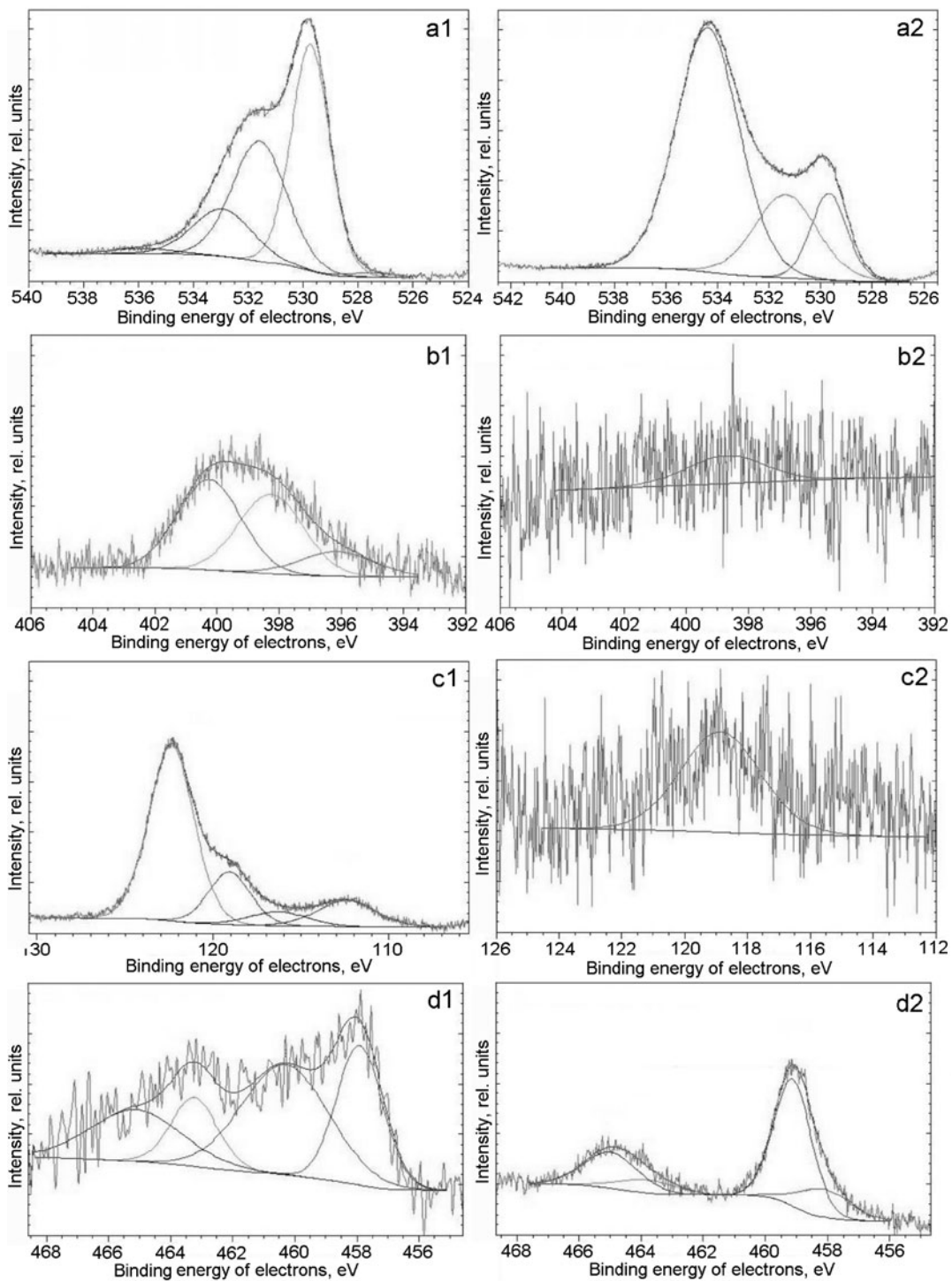
Fig. 5. XP spectra of the composites: a) O1*s* electrons; b) N1*s* electrons; c) Al2*s* electrons; d) Ti2*p* electrons; a1-d1) initial composites; a2-d2) composites after heat treatment.

the samples leads to substantial changes in the spectrum of the N1*s* electrons (Fig. 5, b2). Its intensity decreases sharply, and it is only possible here to identify one signal with $E_b = 400.4$ eV (titanium oxynitride) for the composite with the titanium implant or with $E_b = 398.5$-398.7 eV (implanted nitrogen) for the remaining composites.

TABLE 2. Photocatalytic Oxidation of Benzene (UV)

Composite	Conversion, %					
	1 h reaction			3 h reaction		
	Initial	HT at 300 °C	HT at 500 °C	Initial	HT at 300 °C	HT at 500 °C
Ti/SS	0	2	7	0	9	26
Ti/Mo/SS	0	4	12	2	12	37

For the XP spectra of the implant elements there are series of peculiarities due to the nature of the metal. Thus, for the synthesized composite with implanted aluminum the spectrum of the Al2s electrons (Fig. 5, c1) contains three peaks (against the peak from the Ni2s electrons with E_b = 112.4 eV, nickel oxide). The first of them with E_b = 116.3 eV belongs to metallic aluminum, the second with E_b = 119.4 eV corresponds to the formation of aluminum oxynitride, while the third with S_b = 122.4 eV belongs to aluminum nitride. After heat treatment the spectrum (Fig. 5, c2) contains only one peak with E_b = 118.9 eV, characteristic of aluminum oxide. The formation of this oxide was suggested on the basis of SEM data on the change in the thickness of the layer of implant (see above).

For the initial composite with implanted titanium there are two peaks for the 2$p_{3/2}$ electrons with E_b equal to 460.3 and 457.9 eV (Fig. 5, d1). The first of them with respect to binding energy and spin-splitting constant between the 2$p_{1/2}$ and 2$p_{3/2}$ electrons equal to 4.7 eV, belongs definitely to titanium nitride. The second peak with respect to binding energy and splitting constant, equal to 5.3 eV which is intermediate in value between titanium oxide (5.7 eV) and titanium nitride (4.8 eV), belongs to titanium oxynitride. Heat treatment of the composite leads to substantial changes in the XP spectrum (Fig. 5, d2). The observed peak with E_b = 459.1 eV and splitting constant 5.8 eV belongs to titanium oxide, whereas the second (E_b = 458.1 eV, splitting constant 5.5 eV) belongs to titanium oxynitride. It can be supposed that heat treatment results in oxidation of the titanium oxynitride to its oxide and of titanium nitride to the oxynitride.

For the composite with implanted molybdenum the XP spectrum contains a doublet from the Mo3$d_{5/2}$ and Mo3$d_{3/2}$ electrons with E_b of Mo3$d_{5/2}$ electrons 232.0 eV and spin-spin splitting constant (Mo3$d_{3/2}$–Mo3$d_{5/2}$) equal to 3.2 eV, indicating the presence of only molybdenum oxide MoO$_3$. Heat treatment leads to only a small change in the spectrum (E_b = 231.8 eV, splitting constant 3.15 eV), which indicates no change in the state of the implant on the surface of the composite.

Analysis of the XP spectrum of the Ni2p electrons for the composite with implanted nickel shows the presence of two peaks: the first of them with E_b = 855.3 eV is characteristic of nickel oxide, which is confirmed by the presence of satellites in the spectrum and by the spin-spin splitting constant of 17.5 eV; the second peak with E_b = 858.7 eV belongs to oxynitride structures formed in the surface layer of the composite. Heat treatment of the composite leads to disappearance of the second peak while the position of the first peak changes a little (E_b = 854.9 eV). However, the presence of the satellites and the constancy of the splitting constant indicate the presence of NiO on the surface of the composite.

Thus, the results obtained by XPS have made it possible to establish that the nanosized surface layer of implant formed during implantation of metal ions on the surface of stainless steel consists of oxides, nitrides, and oxynitrides of the metals while the ratio between these compounds is determined by the nature of the implant.

The formation of the nanodimensional coating on the surface of stainless steel during ionic implantation of metal with the simultaneous introducing of part of the implant into the surface layer of the support affects the thermophysical characteristics of the obtained materials. In [27] we showed that when an electric current is passed through a tape of the synthesized composite its surface temperature is higher than the temperature of a standard nichrome heating spiral. (The difference in temperature at a power level of 100 W amounted to 30-50 °C.) Later on we found that with forced delivery of air into the heating zone and with increase of the power of the current the difference in the temperatures of the surface of the

composite and the nichrome increases and at 300 W it amounts to 60-110 °C, depending in the nature of the implant. The metals can be placed in the following order according to the temperature reached under these conditions: Mo (630) > Ti (620) > Al (580) > nichrome (520). It was moreover established that, whereas the temperature of the air during free convection (at a distance of 3 cm from the surface of the spiral) was higher for the nichrome than for the composites, with forced delivery of air (1000 L/h) its temperature changed in the order Ti > Mo > nichrome. This opens up the prospect of using the composites obtained by ionic implantation as heating elements in domestic electric devices.

The prospect of using the obtained composites as supports for the synthesis of active catalysts for the oxidation of methane by the deposition of precious metals was demonstrated in [27] (see above). The authors of [27] also established that the composite itself with implanted nickel exhibits good catalytic characteristics in the conversion of ethanol to hydrogen. Thus, at 450 °C the selectivity with respect to H_2 amounted to 83%-85% with almost complete conversion of the alcohol. Ethylene and acetaldehyde, which can be separated quite easily from the desired product, in addition to CO_2 are present in the reaction products. The efficiency of Al/SS and Ti/SS samples as catalysts in the thermal decomposition of ethanol is established. It was shown that carbon nanotubes are formed in addition to the main product hydrogen. The process occurs for 120 h almost without deactivation of the catalyst, which distinguishes the synthesized composites from the catalysts described in the literature. Further investigations into the use of the composites in catalytic processes established that a high degree of selectivity with respect to acetaldehyde (92%) can be achieved during oxidation of ethanol in the presence of the Mo/SS sample (220 °C, alcohol conversion 99%), which may prove promising for the creation of a new process for the production of this product concurrent with the known Waker process. It was shown that with a sample produced by successive implantation of titanium and molybdenum (Mo/Ti/SS) it was possible to obtain phenol (yield 10-12 mole %) during the gas-phase oxidation of benzene with molecular oxygen. The possibility of using Ti/SS and Ti/Mo/SS in the photocatalytic oxidation of benzene (1200 ppm in water) was studied. The results, presented in Table 2, show almost complete absence of activity in the initial synthesized samples, which may be due to the presence of a significant amount of titanium nitride in the surface layer of the composite (XPS data). After heat treatment of the composite, leading to oxidation of the titanium nitride and formation of a surface layer of titanium oxide and oxynitride (see above), the activity of the composite increases, as mentioned in [30]. It was established that increase of the heat treatment temperature to 600 °C lowers the activity of the catalyst. It can be supposed that the maximum activity is associated with a specific ratio of these two compounds. The activity of the composite is increased by the presence of the intermediate layer of implant, namely, molybdenum oxide (for the composition see above), between the support and the layer of implanted titanium.

The investigation has thus demonstrated experimentally that ionic implantation of metals on the surface of stainless steel leads to the formation of nanodimensional layers of implant, which take the form of X-ray-amorphous compositions consisting of oxides, nitrides, and oxynitrides of the metal. It was found that partial entry of the implant into the subsurface layer of the support leads to the formation of an intermediate layer, and this greatly increases the mechanical and thermal stability of the composites. The prospect of creating new catalysts and supports for various processes, including photoprocesses, by implantation of metals on the surface of various types of supports is discussed.

REFERENCES

1. V. Meille, *Appl. Catal. A*, **315**, 1-17 (2006).
2. J. M. Pout, G. Foti, and D. K. Jacobson, *Modification and Alloying of Surfaces by Laser, Ion, and Electron Beams* [in Russian], Mashinostroenie, Moscow (1987).
3. A. A. Nikitin and N. G. Travina, *Ionic implantation – an Effective Method of Changing the Surface Characteristics of Metals and Alloys* [in Russian], Byul. TsNIICh, No. 23, 9-18 (1986).
4. T. R. Rautray, R. Narayanan, and K. H. Kim, *Progr. Mater. Sci.*, **56**, N 11, 1137-1177 (2011).

5. N. J. Kang, J. G. Kim, H. Y. Lee, et al., *Int. J. Presic. Eng. Man.*, **15**, No. 5, 889-894 (2014).

6. V. A. Zazhigalov and V. V. Goncharov, *Metallofiz. Noveishie Tekhnol.*, **36**, No. 6, 757-766 (2014).

7. *Measurement of Microhardness by Scratching with Diamond Indenters* [in Russian], GOST 21318-75, State Committee of Standards, Council of Ministers of the USSR (1975).

8. V. A. Zazhigalov, *Kinet. Katal.*, **43**, No. 4, 558-565 (2002).

9. V. A. Zazhigalov and E. A. Diyuk, *Teor. Éksp. Khim.,* **54**, No. 1, 61-66 (2018). [*Theor. Exp. Chem.*, **54**, No. 1, 66-72 (2018) (English translation).]

10. A. A. Cherny, S. V. Maschenko, V. V. Honcharov, and V. A. Zazhigalov, *Springer Proc. Phys.*, **167**, 203-213 (2015).

11. J. Dudognon, M. Vayer, A. Pineau, and R. Erre, *Surface Coating Technol.*, **202**, No. 20, 5048-5054 (2008).

12. J. Dudognon, M. Vayer, A. Pineau, and R. Erre, *Surface Coating Technol.*, **203**, No. 1, 180-185 (2008).

13. P. Stefanov, D. Stoychev, A. Aleksandrova, et al., *Appl. Sci.*, **235**, Nos. 1/2, 80-85 (2004).

14. Y. Adraider, Y. X. Pang, F. Nabhani, et al., *Surface Coating Technol.*, **205**, Nos. 23/24, 5345-5349 (2011).

15. V. Honcharov, V. Zazhigalov, Z. Sawlowicz, et al., *Springer Proc. Phys.*, **195**, 355-364 (2017).

16. Z. L. Li, J. Wong-Leung, P. N. K. Deenapanray, et al., *Nucl. Instrum. Methods Phys. Res. B*, **148**, Nos. 1-4, 534-539 (1999).

17. K. Spencer, D. M. Fabijanic, and M. X. Zhang, *Surface Coating Technol*., **206**, No. 14, 3275-3282 (2012).

18. N. Kaur, M. Kumar, S. K. Sharma, et al., *Appl. Surface Sci.*, **328**, 13-25 (2015).

19. F. Luo, W. Ong, Y. Guan, et al., *Appl. Surface Sci.*, **328**, 405-409 (2015).

20. V. D. Parkhomenko and P. N. Tsybulev, *Teor. Éksp. Khim.*, **27**, No. 6, 641-646 (1991). [*Theor. Exp. Chem.*, **27**, No. 6, 555-559 (1991) (English translation).]

21. A. A. Chernyi, S. V. Mashchenko, V. V. Honcharov, and V. A. Zazhigalov, *Khim., Fiz., Tekhnol. Poverkhni*, **5**, No. 2, 190-196 (2014).

22. V. L. Levshunova, G. P. Pokhil, D. I. Tetel'baum, and P. N. Chernykh, *Poverkhnost'*, No. 4, 91-93 (2010).

23. A. W. Kerkar, S. D. Friedman, J. W. Lau, et al., "*Metal foil catalyst members by aqueous electrophoretic deposition,*" PCT, WO 95/32053, IC B 01 J 21/04, 23/02, Publ. Nov. 30, 1995.

24. H. Ota, M. Yashiro, K. Yotsuya, et al., "*Metal catalyst carrier for exhaust gas purification*," USA Pat. 5486338, IC F 01 N 3/10, B 01 D 53/34, Publ. Jan. 23, 1996.

25. S. Sato, K. Oouchi, and K. Nishizawa, *"Metallic catalyst carrier,"* USA Pat. 6761980, IC B 01 J 35/04, Publ. July 13, 2004.

26. C. R. Hatem and B. Colombeau, *"Low temperature ion implantation,"* USA Pat. 2011/0034013, IC B 01 J 35/04, Publ. Feb. 10, 2011.

27. V. A. Zazhigalov, V. V. Goncharov, and I. V. Bacherikova, *Fundamental Problems of Creation of New Substances and Materials of Chemical Production* [in Russian], Akademperiodika, Kiev (2016), pp. 281-290.

28. B. Vincent Crist, *PDF handbooks of monochromatic XPS spectra*, XPS Intern. LLC, 2005, CA, USA. http://www.xpsdata.com.

29. S. Oktay, Z. Kahraman, M. Urgen, and K. Kazmanli, *Appl. Surface Sci.*, **328**, 255-261 (2015).

30. X. Chen, Y. B. Lou, A. C. S. Samia, et al., *Adv. Funct. Mater.*, **15**, No. 1, 41-49 (2005).